CRAMER-RAO BOUNDS FOR
MATCHED FIELD TOMOGRAPHY AND OCEAN ACOUSTIC TOMOGRAPHY

Arthur B. Baggeroer and Henrik Schmidt

Massachusetts Institute of Technology
Cambridge, MA 02139
email: abb@arctic.mit.edu

ABSTRACT

Matched field and ocean acoustic tomography concern the estimation of parameters for models of ocean environments using acoustics. Both require full field representations for the observed signals since waveguide effects are important. We present Cramer-Rao lower bounds for the attainable accuracy of both methods. These bounds are expressed in terms of the Green's function for the propagation between source and receivers.

1. INTRODUCTION

Acoustical methods for determining models of the ocean and its boundaries at the surface and seabed have long been important topics in the geophysical literature. The techniques for taking observed data and producing a model of an ocean environment are described as *inversion algorithms* [1]. Matched field tomography (MFT) and ocean acoustic tomography (OAT) are inverse methods for estimating parameters of models for ocean environments. While the inversion theory literature discusses several performance metrics, the use of Cramer-Rao bounding analysis has not been used extensively especially when compared to its use in the signal processing literature [2]. Nevertheless, several of the methods in geophysical inverse theory which use linearized least squares lead to results similar to those from a Cramer-Rao bound approach.

In OAT a wideband signal is transmitted to receivers where it is matched filtered for the arrival times of the multipaths [3]. These kinematic, or travel time data, are compared to those for models for the propagation and the parameters are iterated to be consistent with the observations. In practice, only kinematic data typically have been used since they have proven to be the most robust of the measurements. OAT has been developed over a span of two decades and it is now an

effective tool for making long term observations which cannot be economically obtained otherwise. Inversion based upon travel time data is also used in a number of geophysical applications; for example, it is the basis of seismic refraction for measuring the crustal structure of the Earth and is now being used in earthquake seismology for the deep Earth structure [5].

MFT is an extension of the source localization problem of matched field processing. [6, 7] In matched field methods one exploits the interference pattern of signals observed on large aperture vertical arrays. For source localization the waveguide nature for the propagation leads to patterns which can be inverted for source range and depth with a resolution better than those attainable with conventional beamforming methods. Most analyses and experiments have been for narrowband signals although a few wideband results are now being reported. Source localization by matched field methods has been demonstrated over the last decade in a number of experiments which have been reported in the acoustical literature. MFT extends this to estimating parameters of an ocean model; however, it is relatively new and experiments to test it are just now underway.

One can contrast how OAT and MFT exploit acoustic signals observed on an array of hydrophones. OAT measures travel times and uses group delays for its observables; as such, it requires a broadband source which is coherent across frequency. In fact, OAT can use purely time domain processing on a single sensor if the arrivals are separated by more the inverse of the source bandwidth; this is how OAT has been principally practiced. MFT requires an array since the inversion is based upon the interference of the phase delays of a signal; however, it does not require coherency across the signal band. Both methods have advantages depending upon the oceanographic conditions influencing the acoustic propagation.

In both tomographic methods the parameters for the ocean are embedded in the observed data so one can apply the bounding techniques to specify attain-

able resolutions. For the bounds to have relevance the signal must be represented with enough fidelity to capture the important features of the propagation. Unfortunately, most of the signal processing literature has used rather simplistic models for the acoustic propagation, so it has not had much relevance to realistic ocean models. Here we import the the wave equation and use full field models for the propagation to derive Cramer-Rao bounds for both tomographic methods. This leads to expressions for the Fisher Information Matrix involving the Green's function which can be efficiently evaluated using acoustic modeling codes.

2. MODEL AND NOTATION

Figure illustrates a model for the seismo/acoustic environment and receiver array. It incorporates the essential features of both OAT and MFT. The figure suggests a range independent environment and hydrophone sensors, but these are not restrictions. The complex
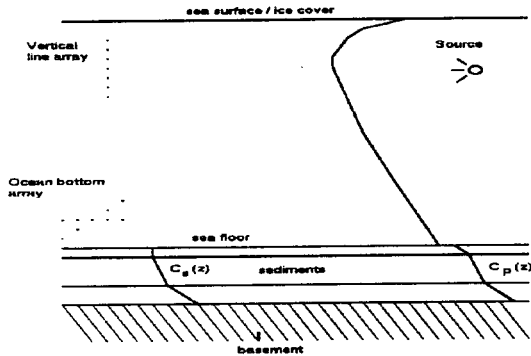

Figure 1: Model for the seismo/acoustic environment, source and receiver arrays.

envelope of the received signal is given by

$$\mathbf{R}(f) = \tilde{b}(f)S_s(f)\mathbf{G}(f, \mathbf{a}) + \mathbf{N}(f, \mathbf{a}), \quad f \in \Delta W; \quad (1)$$

where

$\mathbf{a}$	is a vector of the unknown parameters;
$\mathbf{G}(f, \mathbf{a})$	is a vector of Green's function for the propagation to the receiver array;
$S_s(f)$	is the Fourier transform of a coherent source signal;
$\tilde{b}(f)$	is a random process incorporating amplitude and phase variability;
$\mathbf{N}(f, \mathbf{a})$	is a stationary noise vector with spectral covariance matrix, $\mathbf{K}_n(f, \mathbf{a})$
ΔW	is the frequency band occupied by the signal.

The vector $\mathbf{a}$ can include both source parameters, *e.g.* location and velocity, such as done for matched field localization and environmental parameters, *e.g.* speeds, gradients, densities, orthogonal expansion coefficients, as done for matched field tomography.

The inversions of both OAT and MFT exploit the dependence of the Green's function, $\mathbf{G}(f, \mathbf{a})$, upon the parameter $\mathbf{a}$. In contemporary ocean acoustics the Green's function can be computed in a number of ways which incorporate the waveguide physics [8]. For the analysis here we have used the simplest one for a horizontally stratified ocean waveguide based upon normal modes which is given by [1]

$$\mathbf{G}(f, \mathbf{a}) = \frac{\rho_s e^{-j\pi/4}}{4\pi} \sum_m \frac{\phi_m(z_r, f)\phi_m(z_s, f)}{\sqrt{fp_m(f)R}} e^{-j2\pi f p_m(f)R}$$

where $\phi_m(z, f)$ is the m th mode at the receiver and source depth, $p_m(f)$ is the modal slowness, R is the range and ρ_s the density at the source.

MFT and OAT fit within this model using the following assumptions about the quantities defined above.

1. Matched field tomography: For the matched field source localization and tomography the source signal is a stationary random process; therefore, incoherent across a frequency band. For this we set $S_s(f) = 1$ and let $\tilde{b}(f)$ have the power spectral density, $S_b(f)$. Usually the spectral covariance matrix, $\mathbf{K}_n$ is assumed not to depend upon $\mathbf{a}$. To date, most, but not all, formulations in of the literature have been for a single frequency.

2. Ocean acoustic tomography: For full field ocean acoustic tomography the source is coherent across its frequency band. For this $\tilde{b}(f)$ is a single scalar random variable with variance σ_b^2 and $S_s(f)$ is the source signal, *e.g.* an M sequence or an FM sweep.[2] It also usually assumed that the noise does not depend upon $\mathbf{a}$. In practice, ocean acoustic tomography exploits just travel times of the rays or modes, and not signal amplitudes; as such it is not exactly a full field approach.

3. CRAMER-RAO BOUNDS

The elements of the Fisher Information Matrix, $\mathbf{J}_{i,j}$, for lower bounds upon estimates of the parameter set $\mathbf{a}$ can

[1] There are number of more sophisticated codes for modeling more realistic oceans including range dependence, scattering and elastic media [8].

[2] We introduce a complex Gaussian random amplitude for the source since it is usually more realistic. It both randomizes the phase and allows for an uncertainty in envelope of the source level (2 *dB*)

be found using the above models. Lengthy derivations lead to the following results:

Matched field tomography

$$\mathbf{J}_{i,j} = T \int_{\Delta W} df \, S_b^2(f) \gamma(f, \mathbf{a})$$

$$\times \; [Re\,(d^2(f,\mathbf{a}) l_{i,j}(f,\mathbf{a}) - l_i^\dagger(f,\mathbf{a}) l_j(f,\mathbf{a}))$$

$$+ \; \gamma(f,\mathbf{a})(Re(l_i(f,\mathbf{a})) \, Re(l_j(f,\mathbf{a})) \,)\,] \tag{2}$$

Ocean acoustic tomography

$$\mathbf{J}_{i,j} = \sigma_b^4 \gamma(\mathbf{a})[\; Re\,(d^2(\mathbf{a}) l_{i,j}(\mathbf{a}) - l_i^\dagger(\mathbf{a}) l_j(\mathbf{a}))$$

$$+ \; \gamma(\mathbf{a})\,(Re(l_i(\mathbf{a})) \, Re(l_j(\mathbf{a})) \,)\,] \tag{3}$$

The terms involve integrals over the signal band of several quadratic functions of the Green's function normed by the signal and noise spectra:

$$d^2(f, \mathbf{a}) = \mathbf{G}^\dagger(f,\mathbf{a})\mathbf{K}_n^{-1}(f)\mathbf{G}(f,\mathbf{a});$$

$$d^2(\mathbf{a}) = \int_{\Delta W} |S_s(f)|^2 d^2(f,\mathbf{a}) df;$$

$$l_i(f, \mathbf{a}) = \mathbf{G}^\dagger(f,\mathbf{a})\mathbf{K}_n^{-1}(f)\frac{\partial \mathbf{G}(f,\mathbf{a})}{\partial A_i};$$

$$l_i(\mathbf{a}) = \int_{\Delta W} |S_s(f)|^2 l_i(f,\mathbf{a}) df;$$

$$\tag{4}$$

$$l_{i,j}(f, \mathbf{a}) = \frac{\partial \mathbf{G}^\dagger(f,\mathbf{a})}{\partial A_i}\mathbf{K}_n^{-1}(f)\frac{\partial \mathbf{G}(f,\mathbf{a}_j)}{\partial A_j};$$

$$l_{i,j}(\mathbf{a}) = \int_{\Delta W} |S_s(f)|^2 l_{i,j}(f,\mathbf{a}) df$$

$$\gamma(f,\mathbf{a})) = \frac{2}{1 + S_b(f) d^2(f,\mathbf{a})};$$

$$\gamma(\mathbf{a}) = \frac{2}{1 + \sigma_b^2 d^2(\mathbf{a})}.$$

Each of these terms has a physical interpretation; moreover, in the case of a fully mode resolving array they can be approximated using the derivatives of the phase and group slownesses with respect to the model parameters, the source/receiver range, the center frequency and bandwidth [9].

4. AN EXAMPLE

We consider an example of a 31 element vertical array spanning the water column from $250\ m$ to $1750\ m$ with a 50 m sensor spacing. The nominal ocean model has a Munk profile with an axial depth of 1000 m and an

Cramer Rao bounds

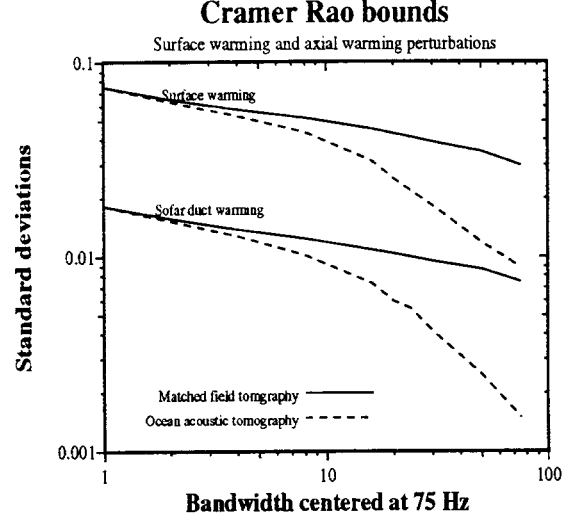Surface warming and axial warming perturbations

Figure 2: Lower bounds for matched field tomography (solid line) and (ocean acoustic tomography (dashed line).

axial sound speed of 1480 m/s [10]. This profile has a shape similar to that indicated in Fig. 1. We introduce two pertubations which are relevant to the use of tomographic methods to monitor ocean in climate. For the first perturbation we have warming at the ocean surface which introduces a profile perturbation of the form

$$\delta c_(z) = \delta c_s e^{-\frac{z}{500}}$$

For the second we have warming at the Sofar axis which we model as

$$\delta c_z = \delta c_a \left(\frac{z}{1000}\right) e^{-\frac{(z-1000)}{1000}}$$

The parameter set for the Cramer-Rao bound is then $\mathbf{a} = (\delta c_s, \delta c_a)$, the surface and axial sound speed perturbations. The range, R, is 1 megameter and the source depth, z_s, is 500 m. The center frequency of the signals is 75 Hz. The noise variance is 10^{-8} which is consistent with for a relative level produced by a 175 dB source and nominal ambient noise levels in the ocean.

We analyze the relative performance of ocean acoustic tomography and matched field tomography as a function of source bandwidth. We constrain the expected transmitted energies for both methods to be equal and constant for all source bandwidths. Figure 2 indicates the results from the Cramer-Rao bounding for the two methods. We see that at low bandwidths both methods have the same performance; however, OAT performs significantly better than MFT for both parameters as bandwidth increases

The performance suggested by the standard deviations from the Cramer Rao are generally consistent with ones physical intuition about the inversion for the two warming models. First, one obtains smaller errors in the Sofar duct than for the surface duct. The array geometry chosen fully spans the Sofar channel but does not go all the way to the surface. In addition, the source couples better to the perturbation of the Sofar axis at this depth.

MFT and OAT exploit bandwidth differently so the decrease in the standard deviations *versus* source bandwidth needs separate considerations. MFT performs an incoherent summation over frequency. The phase interference pattern across the array changes with frequency so the convexity of the matched field processor peak is modulated; consequently, there should be a performance improvement using higher frequencices. This must be traded off *versus* the lower signal level at each frequency since we constrained the total expected transmitted energy for all bandwidths. OAT uses the full bandwidth coherently, so wider bandwidths lead to better travel time resolution and inversion accuracy.

These parameters lead to relatively low SNR's (-20 to -5 *dB*) at the array sensors using a TL (transmission loss) calculation, so the relatively good performance suggested by the Cramer-Rao bound is somewhat surprising even after including an array gain. An explanation for this can be found in the Green's function, $G(f, \mathbf{a})$. The strongest dependence upon the parameter vector, $\mathbf{a}$, is contained in the phase term of the exponent. The bound calculations lead to terms of the form

$$2\pi f \frac{\partial p_m(f, \mathbf{a})}{\partial a_i} R,$$

so there is a very strong amplification of the phase change by the range, R. Since the Cramer Rao bound is basically a perturbation analysis, this amplification is reflected in the performance in much the same way as for frequency modulation systems. (The spatial frequency, $\omega p_m(f, \mathbf{a})$, is in fact being modulated by the perturbation.) This leads to issue of determining if the SNR is adequate for a linearized analysis to be appropriate, *i.e.* is the system above the "threshold" found in most nonlinear modulation systems. To answer this, bounds more appropriate for a threshold analysis need to be used.

5. DISCUSSION

We have introduced the Cramer-Rao bound for comparing ocean acoustic tomography and matched field tomography. These bounds provide a systematic way of comparing the performance of tomographic meth-

ods for ocean acoustics. In particular, array geometries, source center frequencies and bandwidths, and phase (MFP) and travel time (OAT) methods can be compared in a common framework. In the one example calculated we found that OAT out performs MFT under bandwidth and energy constraints.

6. REFERENCES

[1] R. Parker, *Geophysical Inverse Theory*, Princeton University Press, Princeton, N.J., 1994

[2] H. L. Van Trees, *Detection Estimation and Modulation Theory, Parts III*, John Wiley and Sons, 1971

[3] W. H. Munk and C. Wunsch, "Ocean acoustic tomography: a scheme for large scale monitoring," *Deep Sea Research*, 55, pp. 220 -246, 1979

[4] P. F. Worcester, B. D. Cornuelle and R. C. Spindel, " A review of ocean acoustic tomography: 1987 - 1990," *Reviews of Geophysics Supplement*, pp. 557-570, April 1991

[5] K. Aki and P. Richards, *Quantitative Seismology: Theory and Methods*, Freeman Press, New York, 1980

[6] A. B. Baggeroer, W. A. Kuperman and P. N. Mikhalevsky, "An overview of matched field methods in ocean acoustics," *IEEE J. of Oceanic Engineering*, 18(4), pp. 401-424, October 1990

[7] A. Tolstoy, *Matched Field Processing in Underwater Acoustics*, World Scientific Press, Singapore, 1993

[8] F. B. Jensen, W. A. Kuperman, M. Porter and H. Schmidt, *Computational Ocean Acoustics*, American Inst. of Physics Press, New York, 1994

[9] A. B. Baggeroer and H. Schmidt, "Parameter estimation theory bounds and the accuracy of full field inversions," *Proceeding of the NATO Full Field Inversion Workshop* Kluwer Academic Publishers, Dordrecht, The Netherlands (in press)

[10] W. H. Munk, "Sound channel in an exponentially stratified ocean with application to Sofar," *J. of the Acoustical Soc. of Amer.*, 55(2), pp. 220-226, February 1974